Using parity-nonconserving spin-spin coupling to measure the Tl nuclear anapole moment in a TlF molecular beam

John W. Blanchard,[1,2] Dmitry Budker,[1,3,4] David DeMille,[5,6] Mikhail G. Kozlov,[7,8] and Leonid V. Skripnikov[7,9]

[1]*Helmholtz-Institut Mainz, GSI Helmholtzzentrum für Schwerionenforschung GmbH, 55128 Mainz, Germany*
[2]*Quantum Technology Center, University of Maryland, College Park, Maryland 20742, USA*
[3]*Physics, Mathematics, and Computer Science, Johannes Gutenberg-Universität Mainz, 55128 Mainz, Germany*
[4]*Department of Physics, University of California, Berkeley, California 94720-7300, USA*
[5]*Department of Physics, University of Chicago, Chicago, Illinois 60637, USA*
[6]*Physics Division, Argonne National Laboratory, Lemont, Illinois 60439, USA*
[7]*Petersburg Nuclear Physics Institute of NRC "Kurchatov Institute," Gatchina 188300, Russia*
[8]*St. Petersburg Electrotechnical University "LETI," St. Petersburg 197376, Russia*
[9]*Saint Petersburg State University, 7/9 Universitetskaya Naberezhnaya, St. Petersburg 199034, Russia*

(Received 10 November 2022; accepted 1 February 2023; published 20 March 2023)

An experiment utilizing a TlF molecular beam is being developed by the CeNTREX collaboration to search for hadronic interactions that violate both time-reversal ($\mathcal{T}$) and parity ($\mathcal{P}$) invariance. Here, we propose to use the same beam to look for a $\mathcal{T}$-invariance conserving but $\mathcal{P}$-nonconserving (PNC) effect induced by the anapole moment of the Tl nucleus, via a vector coupling of the two nuclear spins in TlF. To measure the nuclear anapole moment, the dc electric and magnetic fields in CeNTREX are replaced by rf fields resonant with a nuclear spin-flip transition. We adapt the relativistic coupled-cluster method in combination with relativistic density functional theory for the calculation of the molecular PNC spin-spin vector coupling constant that links the experimental signal with the anapole moment. The value of the $\mathcal{P}$-conserving spin-spin coupling constant calculated within the same approach is found to be in good agreement with available experimental data.

DOI: 10.1103/PhysRevResearch.5.013191

I. INTRODUCTION

Spatial parity ($\mathcal{P}$) symmetry is violated in weak interactions. Several atomic experiments have been performed to study this phenomenon as reviewed in Refs. [1–4]. The nuclear spin-independent $\mathcal{P}$-odd effect that arises mainly due to the exchange of Z^0 bosons between electrons and the nucleus has been measured several times using atoms and is well established [3]. However, the much smaller nuclear spin-dependent $\mathcal{P}$-odd effects—dominated, for atoms with large atomic number Z, by the interaction of electrons with the nuclear anapole moment—have been observed in atoms only once, with 14% uncertainty [5].

Molecules are promising systems to study parity-nonconserving (PNC) effects [4,6–8], as they have close levels of opposite parity. The small energy interval leads to the mixing of these states by electroweak interactions being amplified. Even so, molecular PNC remains as yet undetected. Various types of molecular experiments have been proposed. A Stark-interference approach was considered and implemented in Refs. [9,10]. It also has been suggested to use the optical rotation technique for diatomic molecules [6,8,11], or to employ enantiomers of chiral molecules [12–24]. Following the proposal in Ref. [25], we consider here another type of experiment to probe the nuclear spin-dependent PNC effect, using a nonchiral molecule. It aims specifically to measure the PNC contribution to the indirect nuclear spin-spin coupling in a diatomic molecule.

To introduce this effect, let us first consider a diatomic molecule with closed electronic shells, with nuclei carrying nonzero nuclear spins $\mathbf{I}$ and $\mathbf{S}$, respectively. In general, the effective Hamiltonian of the indirect interaction of these spins can be written in the following form (we use units with $\hbar = 1$ throughout the paper):

$$H_J = 2\pi I_i J_{ik} S_k. \tag{1}$$

Here, J_{ik} is a reducible rank-2 tensor. The rank-1 contribution is given by

$$H^{(1)} = 2\pi \mathbf{J}^{(1)} \cdot (\mathbf{I} \times \mathbf{S}), \tag{2}$$

where

$$J_i^{(1)} = \tfrac{1}{2}\epsilon_{ijk} J_{jk}^{(1)}, \tag{3}$$

and ϵ_{ijk} is the Levi-Civita tensor. We limit ourselves to the discussion of time-reversal-invariant interactions, so the only option for the $\mathbf{J}^{(1)}$ vector is to be directed along the molecular axis $\boldsymbol{\lambda}$ (a unit vector directed from the heavier nucleus to the lighter one). This is a polar vector, so the resultant interaction

(2) is parity nonconserving. Hence we write

$$H_{\rm PNC} \equiv H^{(1)} = 2\pi J^{(1),{\rm PNC}} \boldsymbol{\lambda} \cdot (\mathbf{I} \times \mathbf{S}), \tag{4}$$

where we write the additional superscript (PNC) to emphasize the parity-violating nature of this term.

Here, we choose the TlF molecule as an example system to discuss the possible measurement of the PNC J-coupling effect. Currently, TlF is used in the Cold Molecule Nuclear Time-Reversal Experiment (CeNTREX) [26,27]. CeNTREX aims to measure the effect induced by the $\mathcal{T},\mathcal{P}$-violating interaction of the nuclear Schiff moment with electrons, with the goal of increasing the sensitivity by three orders of magnitude with respect to the best previous experiment on TlF [28]. In CeNTREX, the measurement scheme is to use an external electric field to orient the molecules along or against the Tl nuclear spin, and then measure the spin-flip energy. The idea of the present proposal is to use similar methods to measure $J^{(1),{\rm PNC}}$, which is induced mainly by the $\mathcal{P}$-odd, $\mathcal{T}$-even nuclear anapole moment of Tl. Below we outline a possible scheme of the experiment and then make estimates of the expected signals and associated sensitivity to PNC. These estimates are based on a precise *ab initio* study of the electronic structure of TlF, with an accurate treatment of the relativistic and electron-correlation effects, which is described here. The expected PNC effect is expressed in terms of the dimensionless constant g characterizing the nuclear anapole moment of the ^{205}Tl nucleus (see Sec. IV A). According to Refs. [2,29], $g(^{205}{\rm Tl}) \approx 0.5$.

II. THE SYSTEM

The ^{205}TlF molecule has closed electronic shells in its ground electronic state ($X\,^1\Sigma^+$). The ground-state levels can be described in terms of the rotational quantum numbers J, M_J and the spins $I = 1/2, M_I$ and $S = 1/2, M_S$ of the ^{205}Tl and ^{19}F nuclei, respectively. The rotational Hamiltonian is $H_{\rm rot} = B\mathbf{J}^2$, and the spins and rotation are coupled via hyperfine interactions, described by the Hamiltonian [27,30,31]

$$H_{\rm HFS} = c_1 \mathbf{I}\cdot\mathbf{J} + c_2 \mathbf{S}\cdot\mathbf{J} + c_3 T^{(2)}(\mathbf{C})\cdot T^{(2)}(\mathbf{I},\mathbf{S}) + c_4 \mathbf{I}\cdot\mathbf{S}. \tag{5}$$

In TlF, the hyperfine couplings c_i are of order kHz while the rotational constant is $B \approx 6.67$ GHz. Here, the third term is the scalar product of two rank-2 tensors, one constructed from two copies of the modified spherical harmonics $\boldsymbol{C}$ and the other from $\mathbf{I}$ and $\mathbf{S}$ [32]. The second-order hyperfine interaction contributes to the third and the fourth terms of the Hamiltonian (5), while the direct dipole-dipole interaction between nuclear magnetic moments contributes only to the third one. An external electric field $\boldsymbol{\mathcal{E}}$ leads to the Stark Hamiltonian $H_{\rm St} = -\mathbf{d}\cdot\boldsymbol{\mathcal{E}} = d\boldsymbol{\lambda}\cdot\boldsymbol{\mathcal{E}}$, where $d = 4.228$ D is the TlF electric dipole moment [33].

For now, we restrict our discussion to TlF levels in the lowest rotational state, $J = 0$. Applying an electric field, $\boldsymbol{\mathcal{E}} = \mathcal{E}\hat{z}$, will electrically polarize the molecule such that the expectation value of the molecular axis direction, $\langle\boldsymbol{\lambda}\rangle = \langle\lambda_z\rangle\hat{z}$, is nonzero (see Fig. 1). The polarization arises, to first order, from a mixture of $J = 1$ odd-parity states into the $J = 0$ even-parity states. For sufficiently small values of $\mathcal{E}$, such that

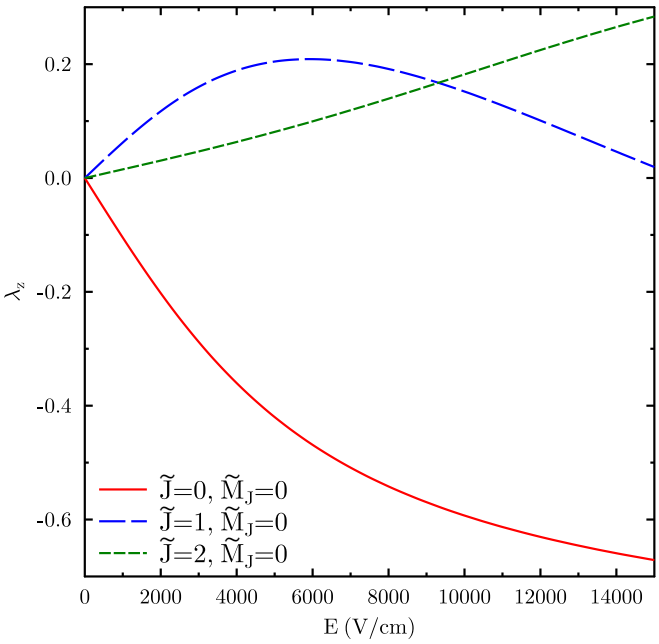

FIG. 1. Polarization $\langle\lambda_z\rangle$ as a function of the electric field, for the lowest J states with $m_J = 0$. The curves are calculated by numerical diagonalization of the rotational + Stark Hamiltonian.

$\mathcal{E} \ll \mathcal{E}_p \equiv B/d$, from perturbation theory it is found that the dimensionless polarization $\langle\lambda_z\rangle$ is linear in $\mathcal{E}$. We define

$$\langle\lambda_z\rangle(\mathcal{E}) \approx \lambda_{z1}(\mathcal{E}/\mathcal{E}_p), \tag{6}$$

where $\lambda_{z1} = -1/(2\sqrt{3})$ from angular factors. In TlF, $\mathcal{E}_p \approx 3.12$ kV/cm [33].

The $|J = 0, M_J = 0\rangle$ state in TlF has four spin sublevels. In a weak $\mathcal{E}$ field such that $J = 0$ remains an approximately good quantum number, the J-dependent terms in Eq. (5), proportional to c_1, c_2, and c_3, vanish. This can be seen from the explicit expression of matrix elements which are diagonal in J for the case of $J = 0$ (see also an explicit form of the matrix element of the term proportional to c_3 in Ref. [31]). The remaining (second-order) hyperfine interaction term $c_4\mathbf{I}\cdot\mathbf{S}$ couples the spin sublevels into a total spin triplet T and a singlet S. We denote these states—including their z-projection quantum numbers M as subscripts—as $|T_0\rangle$, $|T_{\pm1}\rangle$, and $|S_0\rangle$.

Now consider the two-level system $|S_0\rangle$ and $|T_0\rangle$, with nonzero splitting Δ resulting from the hyperfine spin-spin interaction.[1] These levels can be coupled to each other by an external magnetic field, $\boldsymbol{\mathcal{B}} = \mathcal{B}\hat{z}$. In the presence of $\boldsymbol{\mathcal{E}}$, parity mixing due to the Stark interaction induces a nonzero value of $\langle\lambda_z\rangle$, so these states will then also be coupled by the PNC interaction of Eq. (4).

The effective Hamiltonian for the system is then

$$H = \begin{array}{c} \begin{matrix} \langle S_0| & \langle T_0| \end{matrix} \\ \begin{pmatrix} 0 & 0 \\ 0 & \Delta \end{pmatrix} \end{array} + H_Z + H_{\rm PNC}. \tag{7}$$

[1] A small modification to Δ from the Stark interaction is discussed later.

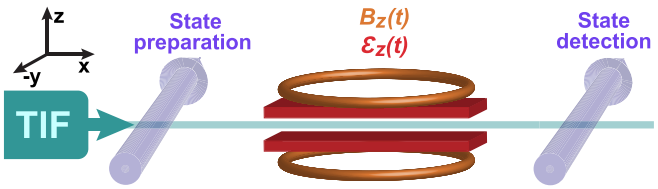

FIG. 2. Schematic diagram of the proposed experiment.

Here, the Zeeman Hamiltonian H_Z may be written as

$$H_Z = -\boldsymbol{\mathcal{B}} \cdot (\gamma_I \mathbf{I} + \gamma_S \mathbf{S}) = \frac{\mathcal{B}}{2}(\gamma_S - \gamma_I), \quad \begin{matrix} \langle S_0| & \langle T_0| \\ \end{matrix} \begin{pmatrix} 0 & 1 \\ 1 & 0 \end{pmatrix}, \tag{8}$$

where γ_I and γ_S are respective gyromagnetic ratios. The effective Hamiltonian (2) for the parity-nonconserving antisymmetric J coupling in the basis of the two considered states has the form

$$H_{\rm PNC} = 2\pi \frac{i\langle \lambda_z \rangle(\mathcal{E})}{2} J^{(1),\rm PNC}(I_+ S_- - I_- S_+) \tag{9}$$

$$= 2\pi \frac{\langle \lambda_z \rangle(\mathcal{E})}{2} J^{(1),\rm PNC}, \quad \begin{matrix} \langle S_0| & \langle T_0| \\ \end{matrix} \begin{pmatrix} 0 & i \\ -i & 0 \end{pmatrix}. \tag{10}$$

Hence, the total Hamiltonian for the system can be written as

$$H = \begin{matrix} \langle S_0| & \langle T_0| \\ \end{matrix} \begin{pmatrix} 0 & \frac{\gamma_{\rm eff}}{2}\mathcal{B} + i\frac{D^{\rm PNC}_{\rm eff}}{2}\mathcal{E} \\ \frac{\gamma_{\rm eff}}{2}\mathcal{B} - i\frac{D^{\rm PNC}_{\rm eff}}{2}\mathcal{E} & \Delta \end{pmatrix}. \tag{11}$$

Here, we have introduced the effective gyromagnetic ratio $\gamma_{\rm eff} = \gamma_S - \gamma_I$ and the effective PNC-induced $E1$ coupling $D^{\rm PNC}_{\rm eff} = 2\pi J^{(1),\rm PNC}\lambda_{z1}/\mathcal{E}_p$.

III. MEASUREMENT SCHEME

A. The simplest case, $J = 0$

The basic idea of the proposed measurement scheme is to determine the effective PNC-enabled $E1$ transition strength $D^{\rm PNC}_{\rm eff}$ between the states $|S_0\rangle$ and $|T_0\rangle$. This can be accomplished by applying an $\mathcal{E}$ field oscillating at frequency $\omega = \Delta$, which will resonantly drive the $|S_0\rangle \leftrightarrow |T_0\rangle$ transition. Measuring the Rabi frequency associated with this drive will determine $D^{\rm PNC}_{\rm eff}$ and hence $J^{(1),\rm PNC}$. As in many other prior or proposed schemes to measure PNC in atoms, the observable effect of the PNC-enabled transition can be amplified through interference with a larger, parity-allowed transition amplitude [34]. Here, we use the $M1$ transition between $|S_0\rangle$ and $|T_0\rangle$ for this purpose.

The beam experiment with TlF molecules may look as follows (see Fig. 2). We prepare the molecule in the singlet state $|S_0\rangle$, so that the wave function of the two-level system is $\Psi_0 = \binom{1}{0}$. Then, each molecule in the beam passes through an interaction region, where oscillating electric and magnetic fields are applied along the z axis: $\mathcal{E}_z(t) = \mathcal{E}_1 \cos\omega t$ and $\mathcal{B}_z(t) = \mathcal{B}_1 \sin\omega t$. We write the time-dependent wave function as $\Psi(t) = \binom{a(t)}{b(t)}$. A given molecule enters the interaction region at time t_0, then, at time $t_0 + T$, exits; we then measure the population $|b(t_0 + T)|^2$ of the triplet state $|T_0\rangle$.

Here, for simplicity, we describe what happens to a monokinetic slice of molecules. (In reality there will be a distribution of molecular velocities, and one would need to average the results correspondingly.) Assuming that we are near the resonance, such that the detuning $\delta = \omega - \Delta$ satisfies $|\delta| \ll |\Delta|$, and applying the rotating-wave approximation, integrating the Schrödinger equation with the Hamiltonian (11) from t_0 to $t_0 + T$ yields the result for the population of the triplet,

$$|b(t_0 + T)|^2 = \frac{\Omega^2_{M1}}{2\Omega'^2}(1 - \cos\Omega' T) - \frac{\Omega_{\rm PNC}\Omega_{M1}}{\Omega'^2} \times \left[\frac{\Omega^2_{M1} T}{2\Omega'} \sin\Omega' T + \frac{\delta^2}{\Omega'^2}(1 - \cos\Omega' T)\right], \tag{12}$$

independent of t_0. Here,

$$\Omega_{\rm PNC} = \frac{D^{\rm PNC}_{\rm eff}}{2}\mathcal{E}_1, \tag{13}$$

$$\Omega_{M1} = \frac{\gamma_{\rm eff}}{2}\mathcal{B}_1, \tag{14}$$

$$\Omega' = \sqrt{\delta^2 + \Omega^2_{M1}}, \tag{15}$$

and we have discarded the small terms quadratic in $\Omega_{\rm PNC}$. The first term in Eq. (12) is independent of $\Omega_{\rm PNC}$, and the second one is linear in $\Omega_{\rm PNC}$. At resonance, where $\delta = 0$ and $\Omega' = \Omega_{M1}$, this expression simplifies to

$$|b(t_0 + T)|^2 = \frac{1}{2}(1 - \cos\Omega_{M1} T) - \frac{\Omega_{\rm PNC} T}{2} \sin\Omega_{M1} T. \tag{16}$$

Throughout this discussion, we have assumed that the level splitting Δ remains constant. However, Stark-induced mixing of the $J = 0$ state with other rotational levels, in combination with hyperfine couplings, causes the value of Δ to change as a function of $\mathcal{E}$: Approximately, Δ in the expressions above should be replaced by

$$\Delta(J = 0) = \Delta_0 + \alpha\mathcal{E}^2 = \Delta_0 + \alpha\mathcal{E}_1^2 \cos^2(\omega t) \tag{17}$$

$$= \Delta_0 + \frac{\alpha}{2}\mathcal{E}_1^2 + \frac{\alpha}{2}\mathcal{E}_1^2 \cos(2\omega t). \tag{18}$$

Under realistic conditions (as discussed below), the frequency modulation depth $\alpha\mathcal{E}_1^2/2$ can be large compared to the linewidth due to the time of flight, $\delta\omega \approx 1/T$. (The dc offset $\alpha/2$ can be accounted for simply by a small change of the driving frequency ω.) It is not immediately obvious that this deep modulation does not dramatically change the outcome described above, when zero modulation was assumed.

In fact, under the conditions we consider here and below, this rapid but seemingly large oscillation of Δ has a negligible

effect on the transition probability. This can be seen as follows. Modulation of the resonant frequency Δ is equivalent to an equal-amplitude (but opposite sign) modulation of the driving frequency ω. A sinusoidal drive frequency modulation of the form $\omega(t) = \omega_0 + \kappa \sin\omega_{\rm mod} t$ is equivalent to a phase modulation, such that the frequency-modulated oscillation $\sin[\omega(t)t]$ can be replaced by $\sin[\omega_0 t + (\kappa/\omega_{\rm mod})\cos\omega_{\rm mod} t]$. In our case, the phase modulation frequency is $\omega_{\rm mod} = 2\omega_0$, and the phase modulation index is $\beta = \alpha\mathcal{E}_1^2/(4\omega_0)$. This is equivalent to driving with a comb of frequencies $\omega_n = \omega_0 \pm n\omega_{\rm mod} = \omega_0(1 \pm 2n)$, with corresponding amplitudes $A_n \propto J_n(\beta)$, where J_n is the Bessel function of order n (see, e.g., Ref. [35]). When $\beta \ll 1$, i.e., when the frequency modulation depth satisfies $\alpha\mathcal{E}_1^2/4 \ll \omega_0$, the amplitude of the fundamental frequency is $J_0(\beta) = 1 + O(\beta^2)$, and that of the nth sideband is $J_n(\beta) \sim \beta^n \ll 1$. Hence the modulation has a negligible effect on the amplitude of the resonant component of the driving field, and only introduces small-amplitude sidebands of far off-resonant driving. That is, its effect is negligible in our scheme.

Now, we return to the main discussion. The $\mathcal{P}$-odd signal arising from Eq. (16) corresponds to the change in the population of the triplet and singlet levels when we reverse the sign of either one (but not both) of the fields $\mathcal{E}_1$ or $\mathcal{B}_1$, since $\Omega_{\rm PNC} \propto \mathcal{E}_1$ and $\Omega_{M1} \propto \mathcal{B}_1$. Fluctuations of the population (the first term independent of $\Omega_{\rm PNC}$) give the noise. Both the signal and the noise turn to zero for $\Omega_{M1}T = 2\pi n$; the signal is maximal when $\Omega_{M1}T = \pi(n + \frac{1}{2})$. We consider the case where both the triplet state population $P_T = |b(t_0 + T)|^2$ and the singlet state population $P_S = 1 - P_T$ are detected, analogous to the plans for detecting both spin quadratures after the Ramsey spin-rotation protocol in CeNTREX [27]. In this case, the PNC signal-to-noise ratio is

$$\mathrm{S/N} = \Omega_{\rm PNC} T\sqrt{N}, \tag{19}$$

where N is the number of detected molecules.

This type of experiment is similar to what was discussed for atomic hydrogen in the 1970s [36,37] and later for alkali metals [38,39]. In these papers, the idea was to look for interference between a PNC-induced $E1$ amplitude and a parity-allowed $M1$ amplitude, driven on resonance between hyperfine sublevels of the same state. Because time-reversal ($\mathcal{T}$) symmetry is conserved, and hence the ratio of the $M1$ and PNC $E1$ amplitudes is pure imaginary [40], these amplitudes can only interfere when the driving $\mathcal{E}$ and $\mathcal{B}$ fields are $\pi/2$ out of phase, as here. Our scheme is also closely related to the proposal by Fortson to measure $E1_{\rm PNC}$-$E2$ interference in a single trapped ion [41]. As discussed there, the S/N is at the standard quantum limit for measuring the ac Stark shift $\Omega_{\rm PNC}$, for N particles observed over coherence time T. Because the resonant frequency Δ is so small here (as compared to all cases in the prior literature), both applied fields are entirely in the near-field regime, with control afforded by simple patterns of conductors and ordinary function generators. We also note that despite some superficial resemblances, the proposed method here is quite different from those used to measure PNC effects in near-degenerate states in Dy [42] and in diatomic molecules [9] such as BaF [10]. In those experiments, the pair of levels considered have opposite parity rather than the same parity as here; the level splitting Δ can be tuned through zero, whereas here it is fixed, and the field driving the system is at a frequency far above resonance, rather than on resonance as here.

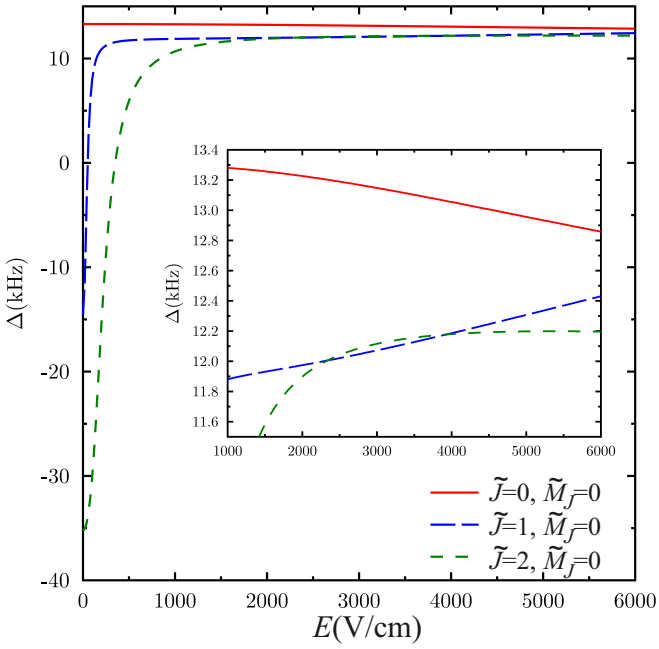

FIG. 3. Splitting Δ for three lowest rotational levels with $\tilde{M}_J = 0$.

B. The $J > 0$ case

The measurement scheme as just described is applicable only to the spin sublevels of the $J = 0$ rotational state. However, it is highly desirable to also perform analogous measurements in states with larger values of J. The reason is that in such states, the slope λ_{z1} of the plot of polarization $\langle\lambda_z\rangle$ vs $\mathcal{E}$ (see Fig. 1) can be of opposite sign to that in the $J = 0$ state. This can provide a powerful means to detect and minimize important systematic errors (see Sec. V). However, for $J > 0$ states in zero $\mathcal{E}$ field, spin-rotation couplings arising from the terms proportional to c_1, c_2, and c_3 in Eq. (5) result in energy eigenstates that are not well described as spin singlet and triplet states. In this regime, our present treatment does not apply and its consideration goes beyond the scope of the present work. However, the triplet-singlet state character can be recovered in the presence of a substantial $\mathcal{E}$ field. Hence, to perform an analogous PNC measurement in states with $J > 0$, we must consider the situation where not only the near-resonant oscillating field $\mathcal{E}_1 \cos\omega t$, but also a large static field $\mathcal{E}_0$, is present. We consider this situation here. Though most of the discussion will be valid for any states with $J > 0$, for concreteness we focus on the case of $J = 1$.

In the presence of a sufficiently large polarizing $\mathcal{E}$ field, such that the Stark energy $d\mathcal{E}$ is large compared to the spin-rotation couplings [arising from the terms proportional to c_1, c_2, and c_3 in Eq. (5)], the spins S and I can decouple from the rotation. In this regime, the vector $\boldsymbol{\lambda}$ rapidly precesses around the electric field $\boldsymbol{\mathcal{E}}$ and the $\mathcal{E}$ field mixes rotational levels of opposite parity (corresponding to J even or odd).

The Stark-split energy eigenstates in the large field regime can be described in terms of approximate quantum numbers $\tilde{J}, \tilde{M}_J$. Here, $\tilde{J}$ corresponds to the value of J that any given state connects to, if the $\mathcal{E}$ field were adiabatically reduced to zero [27]; $\tilde{M}_J$ corresponds to the value of M_J in the limit where all spin-rotation constants vanish. In this regime, states with $\tilde{M}_J = 0$, for any value of $\tilde{J}$, have no diagonal matrix elements of the spin-rotation interactions (to first order in the small ratio $c_j/d\mathcal{E}$). Instead, here—to first order—the hyperfine structure is determined by the spin-spin interaction [i.e., the term proportional to c_4 in Eq. (5)], just as in the field-free $J = 0$ state described above. Hence here, as before, the spin configurations are (to good approximation) singlet and triplet states.

To remain in the large-field regime, the magnitude of the $\mathcal{E}$ field should always remain sufficiently large. To ensure this in the presence of the oscillating $\mathcal{E}$ field used to drive the PNC-induced $E1$ singlet-triplet transition, it is necessary to simultaneously apply a larger dc field. That is, we consider the case where the total applied $\mathcal{E}$ field has the form $\mathcal{E}_0 + \mathcal{E}_1 \cos\omega t$, where $\mathcal{E}_0 > |\mathcal{E}_1|$. In practice, for the $\tilde{J} = 1, \tilde{M}_J = 0$ states in TlF, it is sufficient to maintain $\mathcal{E}_0 - |\mathcal{E}_1| \gtrsim 500$ V/cm.

The primary complication to the PNC measurement arising from the static field $\mathcal{E}_0$ is its effect on the singlet-triplet level splitting Δ. As mentioned earlier, the presence of $J \neq 0$ components of the wave function of every eigenstate—in combination with off-diagonal couplings, due to spin-rotation interactions, with states where $\tilde{M}_J \neq 0$—leads to a shift in Δ. Because the admixtures of different J states into a given $\tilde{J}, \tilde{M}_J = 0$ state change with the size of the applied $\mathcal{E}$ field, Δ also changes with $\mathcal{E}$. The dependence of Δ on $\mathcal{E}$, determined by numerical diagonalization of the full Hamiltonian, is shown in Fig. 3 for states with $\tilde{M}_J = 0$ and $\tilde{J} = 0, 1, 2$. This illustrates clearly the very strong dependence of Δ on $\mathcal{E}$ when $\mathcal{E}$ is small and $\tilde{J} > 0$. However, the dependence weakens for small ranges around sufficiently large values of $\mathcal{E}$. Here, we consider the regime where, in the range $\mathcal{E}_0 - |\mathcal{E}_1| < \mathcal{E} < \mathcal{E}_0 + |\mathcal{E}_1|$, $\Delta(\mathcal{E})$ is approximately a linear function,

$$\Delta(\mathcal{E}_0 + \mathcal{E}_1) \approx \Delta_{\mathcal{E}0} + \alpha' \mathcal{E}_1, \tag{20}$$

where $\Delta_{\mathcal{E}0} \equiv \Delta(\mathcal{E}_0)$. From Fig. 3, for the states with $\tilde{M}_J = 0$ and $\tilde{J} = 1$ ($\tilde{J} = 0$) in TlF, this is a good approximation for $\mathcal{E}_0 \approx 3000$ V/cm and $|\mathcal{E}_1| = 1000$ V/cm. Here, $\Delta_{\mathcal{E}0} \approx 12.1$ kHz (13.1 kHz) and $\alpha' \approx 0.1$ kHz/(kV/cm) [-0.1 kHz/(kV/cm)] for the $\tilde{J} = 1$ ($\tilde{J} = 0$) state. Note also that in this range, the molecular polarization $\langle\lambda_z\rangle$ is approximately linear in $\mathcal{E}$ over the entire range (see Fig. 1).

The Hamiltonian $\tilde{H}$ for this system can be written, in analogy to Eq. (11), as

$$\tilde{H} = \begin{pmatrix} \langle\tilde{S}_0| & \langle\tilde{T}_0| \\ 0 & \frac{\gamma_{\rm eff}}{2}\mathcal{B}_1 \sin\omega t + i\frac{D_{\rm eff}^{\rm PNC}}{2}[\mathcal{E}_0 + \mathcal{E}_1\cos\omega t] \\ \frac{\gamma_{\rm eff}}{2}\mathcal{B}_1 \sin\omega t - i\frac{D_{\rm eff}^{\rm PNC}}{2}[\mathcal{E}_0 + \mathcal{E}_1\cos\omega t] & \Delta_{\mathcal{E}0} + \alpha'\mathcal{E}_1\cos\omega t \end{pmatrix}, \tag{21}$$

where the eigenstates $\langle\tilde{S}_0|$ and $\langle\tilde{T}_0|$ here are the singlet and triplet states when $\mathcal{E} = \mathcal{E}_0$ and the PNC effect is absent. Note that, in this more general situation, the factor $\lambda_{z1}/\mathcal{E}_p$ that appears in the definition of $D_{\rm eff}^{\rm PNC}$ is replaced by the slope of $\langle\lambda_z\rangle$ versus the applied $\mathcal{E}$ field, at the bias field $\mathcal{E}_0$. That is, now $\lambda_{z1}/\mathcal{E}_p \to d\langle\lambda_z\rangle/d\mathcal{E}$, evaluated at $\mathcal{E} = \mathcal{E}_0$. As mentioned above, this slope can be of opposite sign in the $\tilde{J} = 1$ state and the $\tilde{J} = 0$ state, so that $D_{\rm eff}^{\rm PNC}$ is of opposite sign in these states.

Importantly, the off-diagonal matrix elements related to the $\mathcal{E}$ field include *only* PNC couplings. This fact seems far from obvious, given that the eigenstates here are mixed-parity states. A proof of the remarkable fact that ordinary $\mathcal{E}$-field-induced mixing of these states vanishes is given in the Appendix.

Another important observation is that the occupation of the triplet (or singlet) state which is the module square of the solution of the Schrödinger equation with the Hamiltonian (21) is an even function of $\mathcal{B}_1$ (Ω_{M1}) in the absence of PNC effects. This directly follows from the form of the equation. Thus, the modulation of $\Delta_{\mathcal{E}0}$ should not lead to a systematic effect that imitates the PNC signal which is an odd function of $\mathcal{B}_1$ (Ω_{M1}).

As before, by driving the system on resonance ($\omega = \Delta_{\mathcal{E}0}$), applying the rotating-wave approximation, and writing $\tilde{H}$ in the rotating frame, this simplifies to

$$\tilde{H}_{\rm rot} = \begin{pmatrix} \langle\tilde{S}_0| & \langle\tilde{T}_0| \\ 0 & -\frac{i}{2}\Omega_{M1} + \frac{i}{2}\Omega_{\rm PNC} \\ \frac{i}{2}\Omega_{M1} - \frac{i}{2}\Omega_{\rm PNC} & \alpha'\mathcal{E}_1\cos\omega t \end{pmatrix}. \tag{22}$$

The sinusoidal modulation of the level splitting, as before, is equivalent to driving the system with small sidebands at frequencies (here at $\omega_n = \omega \pm n\omega$), and leads to negligible effects. Hence, finally, this system in the presence of the static field $\mathcal{E}_0$ and for a state with any value of $\tilde{J}$ is entirely equivalent to the simpler version discussed before, and the PNC signal can be measured in the same way.

IV. *AB INITIO* CALCULATION OF J-COUPLING PARAMETERS IN TlF

A. Electronic structure theory

Let us now consider parameters that are required to estimate the expected PNC signal (19). Different sources of interactions between the nucleus and electrons in the molecule can induce J coupling (1). Here, we are interested in two of them—the $\mathcal{P}$-even interaction of the electrons with the nuclear magnetic dipole moment and the $\mathcal{P}$-odd interaction with the

anapole moment of the nucleus [43]. The former one has the form

$$H_{\mathrm{HF},K} = \sum_p \gamma_K \frac{\mathbf{I}_K \cdot [(\mathbf{r}_p - \mathbf{R}_K) \times \boldsymbol{\alpha}_p]}{|\mathbf{r}_p - \mathbf{R}_K|^3}, \tag{23}$$

where the summation goes over all electrons of the molecule, $\mathbf{R}_K$ is the position of the nucleus, $\mathbf{r}_p$ is the position of electron p, and $\boldsymbol{\alpha}_p$ are Dirac matrices. The $\mathcal{P}$-odd interactions inside the nucleus K can induce the anapole moment that can be characterized by dimensionless constant g_K. The PNC interaction between the nucleus and electrons induced by this moment is [2]

$$H_{P,K} = \frac{G_\mathrm{F}}{\sqrt{2}} \sum_p g_K \boldsymbol{\alpha}_p \mathbf{I}_K \rho_K(\mathbf{r}_p - \mathbf{R}_K), \tag{24}$$

where $G_\mathrm{F} = 2.222\,49 \times 10^{-14}$ a.u. is the Fermi coupling constant in atomic units and $\rho_K(\boldsymbol{r})$ is the charge density of the nucleus. In addition to the anapole moment there are other contributions to the interaction (24). These contributions can be accounted for by redefining the coupling constant g_K [2].

Interactions (23) and (24) can contribute to the effective Hamiltonian (1) in different combinations. One of them is the parity-conserving indirect coupling of magnetic moments of the nuclei A and B through electronic shells via interactions (23); it will be designated as J^{NMR}. Its components can be calculated as the mixed derivative of the molecular energy E with respect to I and S and with $g_I = 0$, $g_S = 0$:

$$2\pi J^{\mathrm{NMR}}_{ik} = \left.\frac{\partial^2 E}{\partial I_i \partial S_k}\right|_{g_I=0, g_S=0}. \tag{25}$$

In the case of a diatomic molecule oriented along axis z, the tensor J^{NMR}_{ik} has two unique components, $J^{\mathrm{NMR}}_{\perp} = J^{\mathrm{NMR}}_{xx} = J^{\mathrm{NMR}}_{yy}$ and $J^{\mathrm{NMR}}_{||} = J^{\mathrm{NMR}}_{zz}$. It is convenient to use their isotropic combination,

$$J^{\mathrm{NMR}}_{\mathrm{iso}} = (J^{\mathrm{NMR}}_{\parallel} + 2J^{\mathrm{NMR}}_{\perp})/3, \tag{26}$$

and anisotropy,

$$\Delta J^{\mathrm{NMR}} = J^{\mathrm{NMR}}_{\parallel} - J^{\mathrm{NMR}}_{\perp}. \tag{27}$$

$J^{\mathrm{NMR}}_{\mathrm{iso}}$ is the scalar (rank-0) J-coupling part of (1); note that $J^{\mathrm{NMR}}_{\mathrm{iso}} = c_4$ in Eq. (5). The ΔJ^{NMR} constant can be obtained from the experimental value of the c_3 constant [30,31] by subtracting the contribution of the direct interaction of the magnetic dipole moments of Tl and F nuclei, which has been done in Ref. [44].

Components of the J^{PNC}_{ik} tensor that characterize the PNC contribution induced by the anapole moment of the nucleus A to J_{ik} in Eq. (1) can be calculated as

$$2\pi J^{\mathrm{PNC}}_{ik} = \left.\frac{\partial^2 E}{\partial I_i \partial S_k}\right|_{\gamma_I=0, g_S=0}. \tag{28}$$

In TlF, $\mathbf{J}^{(1),\mathrm{PNC}}$ is collinear with the molecular axis. The J^{PNC}_{ik} tensor is antisymmetric. It follows from Eqs. (1)–(3) that $J^{(1),\mathrm{PNC}}_z = J^{\mathrm{PNC}}_{xy}$.

B. Computational details

In the one-particle case and Dirac theory, J^{NMR}_{ik} can be calculated using the operator (23) within the sum-over-states approach:

$$2\pi J^{\mathrm{NMR}}_{ik} = \sum_n \frac{\langle 0|\gamma_I \frac{[(\mathbf{r}-\mathbf{R}_I)\times\boldsymbol{\alpha}]_i}{|\mathbf{r}-\mathbf{R}_I|^3}|n\rangle\langle n|\gamma_S \frac{[(\mathbf{r}-\mathbf{R}_S)\times\boldsymbol{\alpha}]_k}{|\mathbf{r}-\mathbf{R}_S|^3}|0\rangle}{E_0 - E_n} + \mathrm{c.c.} \tag{29}$$

In this equation, the sum goes over positive- and negative-energy states, excluding the occupied one-particle state $|0\rangle$. Below we will distinguish the positive- and negative-energy parts of Eq. (29). J^{PNC}_{xy} can be calculated in a similar way for the one-particle case:

$$2\pi J^{\mathrm{PNC}}_{xy} = \sum_n \frac{\langle 0|\frac{G_\mathrm{F}}{\sqrt{2}} g_I \alpha_x \rho_I(\mathbf{r}-\mathbf{R}_I)|n\rangle\langle n|\gamma_S \frac{[(\mathbf{r}-\mathbf{R}_S)\times\boldsymbol{\alpha}]_y}{|\mathbf{r}-\mathbf{R}_S|^3}|0\rangle}{E_0 - E_n} + \mathrm{c.c.} \tag{30}$$

The simplest generalization of Eqs. (29) and (30) on the many-electron case requires summing also over all occupied molecular bispinors, i.e., replacing $|0\rangle$ by the sum over all occupied $|i\rangle$. This is the so-called uncoupled approximation and will be referenced as PT2. In a more accurate treatment, one can use the linear-response technique developed for both the Dirac-Hartree-Fock (DHF) and density functional theory (DFT) approaches to calculate the components of J coupling and other NMR properties [21,22,45–48]. This approach corresponds to the "analytical" treatment of derivatives (25) and (28) at the DHF and DFT levels instead of simple summations in (29) and (30). For example, within the linear-response DHF method [47], one obtains the following closed-form expression for J^{PNC}_{xy},

$$2\pi J^{\mathrm{PNC}}_{xy} = \sum_{k,l,a,b} \langle k|\frac{G_\mathrm{F}}{\sqrt{2}} g_I \alpha_x \rho_I(\mathbf{r}-\mathbf{R}_I)|a\rangle P^{-1}_{a,k;b,l} \langle b|\gamma_S \frac{[(\mathbf{r}-\mathbf{R}_S)\times\boldsymbol{\alpha}]_y}{|\mathbf{r}-\mathbf{R}_S|^3}|l\rangle + \mathrm{c.c.},$$

where

$$\mathbf{P}^{-1} = \begin{bmatrix} \mathbf{A} & \mathbf{B}^* \\ \mathbf{B} & \mathbf{A}^* \end{bmatrix}^{-1},$$

$$A_{k,l,a,b} = \delta_{a,b}\delta_{k,l}(E_a - E_k) + \langle al|g|kb\rangle - \langle al|g|bk\rangle,$$

$$B_{k,l,a,b} = \langle kl|g|ab\rangle - \langle kl|g|ba\rangle.$$

In the expression above, k, l run over occupied orbitals, a, b run over virtual positive- and negative-energy orbitals, E_k, E_a are corresponding orbital energies, and g is the electron-electron Coulomb operator. The positive-energy state contribution can be obtained by restricting a, b above by the

positive-energy virtual orbitals only. We define and calculate the "negative-energy contribution" in the many-electron case as the difference between the total linear-response value (i.e., with no restrictions applied on indices a, b) for derivatives (25) or (28) and the corresponding positive-energy state contribution. One can see that neglecting two-electron integrals $\langle\cdots|g|\cdots\rangle$ in the expression above leads to the PT2 approach. Below we will call the linear-response DHF or DFT methods just DHF or DFT. The positive-energy part of the related property, a shielding tensor for a molecule containing a heavy atom, can be calculated with a smaller uncertainty than DHF/DFT within the relativistic coupled-cluster theory [49–51]. Here, we have generalized this approach to calculate PNC and $\mathcal{P}$-conserving contributions to the nuclear indirect spin-spin coupling. For this we have numerically calculated mixed derivatives (25) and (28) for the energy E obtained within the coupled-cluster theory. In the used procedure we obtained a set of occupied and virtual orbitals within the molecular Dirac-Hartree-Fock method for TlF. After that, the interactions (23) and (24) were added to the electronic Hamiltonian and coupled-cluster calculations were performed to obtain the positive-energy contribution.

All molecular calculations have been performed within the Dirac-Coulomb Hamiltonian. We have used the combinations of Dyall's Gaussian-type basis sets. For example, the TZTZ basis set corresponds to the uncontracted augmented all-electron triple-zeta Dyall's AAETZ basis set for both Tl and F atoms [52–54] (thus basis sets on both atoms are of the triple-zeta quality, which is implied in the "TZTZ" abbreviation above; similar abbreviation are used below), while TZQZ corresponds to the AAETZ basis set for Tl and augmented all-electron quadruple-zeta AAEQZ for F, etc. In all-electron (90e) correlation calculations within the coupled-cluster with single- and double-cluster amplitudes method (CCSD), we have not used any truncation of the virtual orbitals by their energies. To consider the contribution of high-order correlation effects at the level of coupled cluster with single, double, and triple amplitudes (CCSDT) we have performed correlation calculations for 20 valence electrons and set the cutoff for virtual orbitals energies to $30E_H$, and used the double-zeta (DZ) quality basis set for both atoms with the extended number of s- and p-type functions for both Tl and F. This basis set will be called DZDZext. For calculation of the negative-energy contribution, we have also used the relativistic density functional theory with the hybrid Perdew-Burke-Ernzerhof PBE0 functional [55].

For the problem under consideration, the basis set for all-electron coupled-cluster calculations should include functions with large exponential parameters to accurately reproduce the wave-function asymptotic near and inside the nucleus. The most important here are $s_{1/2}$- and $p_{1/2}$-type functions which can penetrate inside the nucleus. We have found that for the fluorine atom the saturation is achieved if one includes s and p basis functions corresponding to the AAEQZ [52–54] basis set. Therefore, we have used this basis set for fluorine in the main calculations of J-coupling contributions. At the same time for the thallium atom a rather accurate description is achieved already for the AAETZ [52–54] basis set.

In all calculations, the experimental internuclear distance R(Tl-F) = 3.94 bohrs [56] has been employed. For the nuclear magnetic moments we used the values from Ref. [57]: $\mu(^{205}\mathrm{Tl}) = 1.638\,21\mu_N$, $\mu(^{19}\mathrm{F}) = 2.628\,87\mu_N$.

We have used the Gaussian model for the nuclear charge distribution which is well suited for molecular calculations [58]. Relativistic four-component calculations have been performed within the locally modified DIRAC [48,59] and MRCC [60] codes. For calculation of matrix elements of operators (23) and (24) the code developed in Refs. [61–63] was used.

TABLE I. Isotropic and anisotropic components (in Hz) of $\mathcal{P}$-conserving indirect nuclear spin-spin coupling in $^{205}\mathrm{Tl}^{19}\mathrm{F}$.

Contribution	$J_{\mathrm{iso}}^{\mathrm{NMR}}$	ΔJ^{NMR}
Negative-energy state contributions		
DHF-uncoupled (PT2)/QZQZ	0	189
DHF/QZQZ	0	188
DFT/QZQZ (total negative)	0	191
Positive-energy state contributions		
DHF/TZQZ	−27582	11647
DFT/TZQZ	−15462	13123
90e-CCSD/TZQZ	−13586	9820
+20e-(CCSDT-CCSD)/DZDZext	122	867
Total positive	−13463	10687
Total	−13463	10877
Experiment [30,31,44]	−13300(700)	11100(500)

C. Results and discussion of calculation

Table I gives the calculated values of the parity-conserving indirect nuclear spin-spin coupling tensor components (26) and (27) in comparison with the experimental values [30,31,44]. We have found that the negative-energy state contributions to J_{ik}^{NMR} calculated within the linear-response DHF, DFT, or uncoupled DHF (PT2) coincide within a few Hz. Similar behavior has been found for the shielding constant [49]. However, the positive-energy state contribution strongly depends on the level of the theory to treat correlation effects. It can be seen that the value of the anisotropy obtained within the density functional theory deviates from the experimental value by about 20%. Therefore, we have used the relativistic four-component coupled-cluster approach to calculate the positive-energy $\mathcal{P}$-conserving contribution. As it can be seen from Table I, such an approach provides rather accurate values of both isotropic and anisotropic components of J^{NMR}.

Table II gives the calculated values of the PNC contribution to the indirect nuclear spin-spin coupling $J^{(1),\mathrm{PNC}}$ (4).

It can be seen that the leading contribution to this coupling is due to negative-energy states. This contribution is practically the same for the linear-response DHF, DFT, or uncoupled DHF (PT2). In contrast, the positive-energy contribution to $J^{(1),\mathrm{PNC}}$ strongly depends on the level of the electronic correlation treatment, even more strongly than the $\mathcal{P}$-conserving term, e.g., the DFT value is four times smaller than the DHF value. The explicit treatment of electron correlation effects within the relativistic coupled-cluster approach with single and double amplitudes leads to even stronger suppression of the positive-energy contribution. The inclusion of triple cluster amplitudes gives a small, but non-negligible,

TABLE II. PNC contribution to J coupling, $J^{(1),\mathrm{PNC}}$, in $^{205}\mathrm{Tl}^{19}\mathrm{F}$ induced by the anapole moment of the $^{205}\mathrm{Tl}$ nucleus.

Contribution	Value, $10^{-3} g_{\mathrm{Tl}}$ Hz
Negative-energy state contributions	
DHF-uncoupled (PT2)/QZQZ	−2.82
DHF/QZQZ	−2.82
DFT/QZQZ (total negative)	−2.83
Positive-energy state contributions	
DHF/TZQZ	−2.05
DFT/TZQZ	−0.52
90e-CCSD/TZQZ	−0.13
+ 20e-(CCSDT-CCSD)/DZDZext	−0.07
Total positive	−0.19
Total	−3.03

contribution compared with the total positive-energy one. It can be seen that the density functional theory considerably overestimates the positive-energy contribution. A similar overestimation has been also outlined in Ref. [22]. Note that the total positive-energy contribution calculated at the coupled-cluster level itself is more than an order of magnitude smaller than the negative-energy one. According to our estimates, the final uncertainty of $J^{(1),\mathrm{PNC}}$ given in Table II is less than 8%.

The final value of $|J^{(1),\mathrm{PNC}}|$ is of the same order as the estimation obtained in Ref. [25], $9 \times 10^{-3} g_{\mathrm{Tl}}$ Hz. The equation that has been used in Ref. [25] to estimate $J^{(1),\mathrm{PNC}}$ can be obtained from the equation similar to Eq. (30) with consideration of only the negative-energy contribution and some further approximations [25]: setting $|1s(\mathrm{Tl})\rangle$ as $|0\rangle$, replacement of $(E_0 - E_n)$ by $2mc^2$, and replacement of the $\sum_n |n\rangle\langle n|$ by 1. A similar approach for the diamagnetic contribution to the shielding constant is known as the Sternheim's approximation [47,64]. It is instructive to calculate the following sum,

$$2\pi J_{xy}^{\mathrm{PNC}} = \sum_n{}' \frac{\langle 1s|\frac{G_{\mathrm{F}}}{\sqrt{2}} g_I \alpha_x \rho_I(\mathbf{r}-\mathbf{R}_I)|n\rangle\langle n|\gamma_S \frac{[(\mathbf{r}-\mathbf{R}_S)\times\boldsymbol{\alpha}]_y}{|\mathbf{r}-\mathbf{R}_S|^3}|1s\rangle}{2mc^2} + \mathrm{c.c.}, \tag{31}$$

where $|1s\rangle$ is the lowest positive-energy molecular bispinor obtained within the Dirac-Hartree-Fock approach and the summation over $|n\rangle$ includes only the negative-energy states. The obtained value in this approximation, $-8.9 \times 10^{-3} g_{\mathrm{Tl}}$ Hz, almost coincides with the result of Ref. [25]. If one further includes a summation over all occupied bispinors $|i\rangle$ (instead of only $|1s\rangle$), then the value is $-10.9 \times 10^{-3} g_{\mathrm{Tl}}$ Hz. However, if one further uses the actual values of $(E_i - E_n)$ instead of the $(E_i - E_n) \approx 2mc^2$ approximation, then we come to the "PT2" value for the negative-energy contribution given in the first line of Table II, i.e., about the three times smaller value $-2.82 \times 10^{-3} g_{\mathrm{Tl}}$. It means that the approximation $(E_i - E_n) \approx 2mc^2$ used previously overestimates the effect. In other words, negative-energy states for which $(E_i - E_n) \gg 2mc^2$ also contribute to the considered PNC effect. More specifically, according to our analysis within the PT2 approach, negative-energy states $|n\rangle$ whose energy gap between the E_n energy and the energy of the first occupied positive-energy state are smaller than $3mc^2$ give about 46% of the total negative-energy states contribution; negative-energy states with an energy gap smaller than $6mc^2$ contribute 72%; negative-energy states with a gap smaller than $13mc^2$ contribute 91%. The remaining part of the effect (9%) is due to states with a higher-energy gap. Such behavior can be explained by the localization of the PNC operator (24) inside the nucleus.

Substituting an estimation $g(^{205}\mathrm{Tl}) \approx 0.5$ [2,29] to the final value of $J^{(1),\mathrm{PNC}}$ in terms of $g(^{205}\mathrm{Tl})$, one obtains $|J^{(1),\mathrm{PNC}}| \approx 1.5$ mHz.

V. CONSIDERATIONS FOR AN EXPERIMENT WITH TlF

Let us estimate the PNC signal for the apparatus and the beam used in the CeNTREX experiment [27]. The length of the working region there is $L = 2.5$ m and the averaged beam velocity is $\langle v_z \rangle = 184$ m/s. This gives us an interaction time $T = 14$ ms. The coefficient in the Zeeman term (8) is

$$(\gamma_I - \gamma_S) \approx 2\pi(-1.5\ \mathrm{kHz/G}). \tag{32}$$

This means that to have $\Omega_{M1} T = \frac{\pi}{2}$, we need $\mathcal{B}_1 \approx 24$ mG.

To estimate the signal for $\tilde{J} = 0$ in the presence of the static and oscillating electric fields with amplitudes $\mathcal{E}_0 \approx 3000$ V/cm and $\mathcal{E}_1 = 1000$ V/cm we use the value $d\langle\lambda_z\rangle/d\mathcal{E}|_{\mathcal{E}_0}\mathcal{E}_1 = 0.079$ calculated for this field (see Fig. 1). In this case $\Omega_{\mathrm{PNC}}(\tilde{J}=0) \approx 0.37 \times 10^{-3}\ \mathrm{s}^{-1}$. For the case of $\tilde{J} = 1$ and the same fields $\Omega_{\mathrm{PNC}}(\tilde{J}=1) \approx -0.17 \times 10^{-3}\ \mathrm{s}^{-1}$.

In the CeNTREX experiment it is anticipated to detect $N_d \approx 6 \times 10^8$ molecules per pulse [27]. Now we can use Eq. (19) to estimate the statistical sensitivity of the proposed experiment. To reach the ratio S/N = 1 for $\tilde{J} = 0$, one needs a number of pulses N_p given by

$$N_p = \frac{1}{(\Omega_{\mathrm{PNC}} T)^2 N_d} \approx 62\ \mathrm{pulses}, \tag{33}$$

or about 1.24 s at the anticipated repetition rate of 50 Hz. In about 3.5 h one can accumulate S/N = 100. We conclude that the statistical sensitivity of the proposed experiment is easily sufficient for an accurate measurement of the anapole moment of the thallium nucleus.

A detailed analysis of the possible systematic effects is still to be done. However, we point out that PNC experiments use reversals of experimental parameters to isolate the effect of interest from systematics, and two primary reversals are available in this case. These are (i) reversal of the phase (i.e., sign flip) of the oscillating $\mathcal{E}$ field and (ii) reversal of the phase (i.e., sign flip) of the oscillating $\mathcal{B}$ field. With only these two reversals, a possible systematic effect of concern is the following. Applying the oscillating electric field will lead to correlated charging currents and likely a component of magnetic field out of phase with the electric field. If this charging-current $\mathcal{B}$ field has a component along $\mathbf{z}$, it will add to/subtract from the deliberately applied oscillating $\mathcal{B}$ field and hence change the magnitude of Ω_{M1} when the phase of the $\mathcal{E}$ field is reversed. This will exactly mimic the signature of the PNC signal. To combat this effect, we can make measurements not only on the rotational state $\tilde{J} = 0$, but also on $\tilde{J} = 1$. In these two cases,

the $M1$ transition matrix elements are nearly the same, while the PNC signal is of opposite sign due to the opposite direction of the polarization of these states in the electric field (Fig. 1) as discussed above. Hence a properly weighted difference of the results from the two rotational states will cancel the charging-current effect but preserve the PNC effect.

An accurate determination of the coupling constant $g_{\rm Tl}$ for the two stable isotopes (^{203,205}Tl) will allow one to study different contributions to this constant. Within the standard model, this constant is determined by the strength of nucleon-nucleon parity-violating weak interactions [65,66], which remain poorly understood [67]. Two prior measurements of $g_{\rm Tl}$ based on the detection of parity-violating optical rotation in Tl atoms [68,69] gave results consistent with zero, but with uncertainties comparable to the anticipated value $g(^{205}\text{Tl}) \approx 0.5$ [2,29]. More accurate measurements of the nuclear anapole moment will provide additional information on PNC nuclear forces [70]. In addition, such an experiment will be sensitive to spin-dependent interactions with bosonic dark matter, which is predicted by some models. One of them considers an interaction of nucleons with a hypothetical static pseudovector cosmic field [71]. The constraint on the proton-cosmic field interaction parameter b_p^0, currently obtained [71] from the limits on the ^{203,205}Tl anapole moment [68,69], can be improved when the constant $g_{\rm Tl}$ is measured as proposed here. Another prospect is to study a possible contribution due to hypothetical light vector bosons [72]. The nuclear spin-independent parity-violation effects due to such beyond-the-standard-model bosons were recently constrained in atomic parity-violation measurements in a chain of Yb isotopes [73].

VI. CONCLUSIONS

Indirect electron-mediated interactions between two nuclear spins in a diatomic molecule provide an attractive route towards the measurement of long sought-after molecular PNC. The technique is especially promising since, as demonstrated in the present work, (i) the PNC effect is predicted to be large enough to be measured in an ongoing experiment (CeNTREX) and (ii) it can be reliably calculated. This opens a clear path to measuring the nuclear anapole moments of the two stable isotopes, ^{205}Tl and ^{203}Tl, a result that would be of high importance for understanding weak interactions within nuclei [65,66] and in the search for additional vector bosons [72], as well as possible cosmic fields that may be related to the "dark sector" [71].

ACKNOWLEDGMENTS

Electronic structure calculations have been carried out using the computing resources of the federal collective usage center Complex for Simulation and Data Processing for Mega-science Facilities at National Research Centre "Kurchatov Institute" [74], and partly using the computing resources of the quantum chemistry laboratory. The authors are grateful to Victor Ezhov and Vladimir Ryabov for useful comments about the possible experimental setup, and to Olivier Grasdijk and Oskari Timgren for helpful simulations of toy models. This work was supported in part by the Deutsche Forschungsgemeinschaft (DFG – German Research Foundation) Project ID 390831469: EXC 2118 (PRISMA+ Cluster of Excellence) and Project ID 423116110, and in part by Argonne National Laboratory. L.V.S. acknowledges support by the Russian Science Foundation under Grant No. 19-72-10019 for calculations of J-coupling tensor components performed at NRC "Kurchatov Institute" – PNPI and also acknowledges the support of the foundation for the advancement of theoretical physics and mathematics "BASIS" grant according to Project No. 21-1-2-47-1 for the selection rules analysis and calculation of electric field dependence of PNC matrix elements performed at SPbU.

APPENDIX: VANISHING ELECTRIC DIPOLE MATRIX ELEMENT BETWEEN $\tilde{S}_0$ AND $\tilde{T}_0$ STATES

Below we show that there is no coupling by an additional $\mathcal{E}$ field of mixed-parity singlet $|\tilde{S}_0\rangle$ and triplet $|\tilde{T}_0\rangle$ states in the absence of the PNC effect. For this, let us consider eigenfunctions $|F, p, M_F\rangle$ of the field-free Hamiltonian

$$H_0 = B\mathbf{J}^2 + c_1\mathbf{I}\cdot\mathbf{J} + c_2\mathbf{S}\cdot\mathbf{J} + c_3 T^{(2)}(\mathbf{C})\cdot T^{(2)}(\mathbf{I},\mathbf{S}) + c_4\mathbf{I}\cdot\mathbf{S}, \tag{A1}$$

which conserves quantum numbers F, p, and M_F, where F is the value of the total angular momentum $\mathbf{F} = \mathbf{J} + \mathbf{I} + \mathbf{S}$, M_F is the projection of $\mathbf{F}$ on the laboratory axis, and p is the spatial parity. We are interested in wave functions with $M_F = 0$. For the considered case of $I = 1/2$ and $S = 1/2$ they can be written in the basis of functions with definite F and J quantum numbers as well as the total spin of Tl and F nuclei designated as R_{IS}:

$$\begin{aligned}|F, p, M_F = 0\rangle = {} & e|F, J = F+1, R_{IS} = 1, M_F = 0\rangle \\ & + f|F, J = F-1, R_{IS} = 1, M_F = 0\rangle \\ & + g|F, J = F, R_{IS} = 1, M_F = 0\rangle \\ & + h|F, J = F, R_{IS} = 0, M_F = 0\rangle.\end{aligned} \tag{A2}$$

Coefficients e, f, g, h depend on the parameters of H_0. However, for a given parity p, only one of the pairs of coefficients e, f or g, h is nonzero, i.e., there are two classes of eigenfunctions of H_0 with opposite parities. Each basis function in Eq. (A2) can be further expressed in terms of the following uncoupled spin-rotational functions

$$|J, S_0\rangle = \frac{1}{\sqrt{2}}|J, M_J = 0\rangle(|\uparrow_I\downarrow_S\rangle - |\downarrow_I\uparrow_S\rangle), \tag{A3}$$

$$|J, T_0\rangle = \frac{1}{\sqrt{2}}|J, M_J = 0\rangle(|\uparrow_I\downarrow_S\rangle + |\downarrow_I\uparrow_S\rangle), \tag{A4}$$

$$|J, T_{-1}\rangle = |J, M_J = 1\rangle|\downarrow_I, \downarrow_S\rangle, \tag{A5}$$

$$|J, T_1\rangle = |J, M_J = -1\rangle|\uparrow_I, \uparrow_S\rangle, \tag{A6}$$

using standard angular momentum algebra [75]. By applying this expansion we arrive at the following eigenfunctions of H_0 with definite parities,

$$\begin{aligned}|\Phi_s\rangle &= |F, p = (-1)^F, M_F = 0\rangle \\ &= \alpha_J|J, S_0\rangle + \beta_J(|J, T_1\rangle - |J, T_{-1}\rangle), J = F,\end{aligned} \tag{A7}$$

$$|\Phi_t\rangle = |F, p = (-1)^{F+1}, M_F = 0\rangle$$
$$= \sum_{J=F\pm1} \gamma_J |J, T_0\rangle + \delta_J(|J, T_1\rangle + |J, T_{-1}\rangle), \quad \text{(A8)}$$

where the coefficients α_J, β_J, γ_J, δ_J are determined by parameters of the Hamiltonian H_0.

Now let us consider the case with an applied uniform external electric field along the laboratory axis, i.e.,

$$H_{\text{stat.}} = H_0 + d\mathcal{E}_0 \cos\theta, \quad \text{(A9)}$$

where θ is the angle between the molecular and laboratory axes. In the present case M_F is still a good quantum number while F and p are not. Eigenfunctions of this Hamiltonian in a given basis set can be obtained by its diagonalization. Let us calculate the following matrix element of interest in the basis of eigenfunctions of the unperturbed Hamiltonian H_0 considered above:

$$\langle\Phi_s|H_{\text{stat.}}|\Phi'_t\rangle = \langle\Phi_s|d\mathcal{E}_0\cos\theta|\Phi'_t\rangle = \langle F, p = (-1)^F, M_F = 0|d\mathcal{E}_0\cos\theta|F', p' = (-1)^{F'-1}, M_F = 0\rangle$$
$$= \sum_{J'=F'\pm1} \beta_J\delta_{J'}(\langle J = F, T_1|d\mathcal{E}_0\cos\theta|J', T_1\rangle - \langle J = F, T_{-1}|d\mathcal{E}_0\cos\theta|J', T_{-1}\rangle) = 0. \quad \text{(A10)}$$

In the last equality we have used Eqs. (A5) and (A6) and the property $\langle J, M_J|\cos\theta|J', M_J\rangle = \langle J, -M_J|\cos\theta|J', -M_J\rangle$. Note also that these matrix elements are nonzero only for $J = J' \pm 1$, but in any case they either cancel each other out or both vanish in Eq. (A10). Thus, the matrix of the Hamiltonian $H_{\text{stat.}}$ in the considered basis set is quasidiagonal and after its diagonalization the resulting eigenfunctions will not have a mixture of Φ_s and Φ'_t functions for any external electric field $\mathcal{E}_0$, i.e., resulting electric field-dependent functions $\tilde{\Phi}_s$ will be linear combinations of only $\{\Phi_s\}$ functions (A7) with various F, while electric field-dependent functions $\tilde{\Phi}_t$ will be linear combinations of only $\{\Phi_t\}$ (A8). According to Eq. (A10) there would be no coupling by an additional $\mathcal{E}$ field of mixed-parity singlet $|\tilde{S}_0\rangle$ and triplet $|\tilde{T}_0\rangle$ states. Note that this result also holds for the more general case when additional parity-conserving interactions inside the molecule (e.g., nonadiabatic ones) are included in the Hamiltonian. This follows from the symmetry arguments. In the static uniform external electric field the system has a group of symmetry $C_{\infty v}$ with the axis of symmetry along the laboratory axis. Functions $\tilde{\Phi}_s$ and $\tilde{\Phi}_t$ transform according to different irreducible representations Σ^+ and Σ^- of this group, respectively, and cannot be coupled by the operator $\sim z$, transforming according to the Σ^+ irreducible representation.

[1] M.-A. Bouchiat, Atomic parity violation. Early days, present results, prospects, Nuovo Cimento C **35**, 78 (2012).

[2] J. S. M. Ginges and V. V. Flambaum, Violations of fundamental symmetries in atoms and tests of unification theories of elementary particles, Phys. Rep. **397**, 63 (2004).

[3] M. S. Safronova, D. Budker, D. DeMille, D. F. J. Kimball, A. Derevianko, and C. W. Clark, Search for new physics with atoms and molecules, Rev. Mod. Phys. **90**, 025008 (2018).

[4] I. B. Khriplovich, *Parity Non-Conservation in Atomic Phenomena* (Gordon and Breach, New York, 1991).

[5] C. Wood, S. Bennett, D. Cho, B. Masterson, J. Roberts, C. Tanner, and C. E. Wieman, Measurement of parity nonconservation and an anapole moment in cesium, Science **275**, 1759 (1997).

[6] O. P. Sushkov and V. V. Flambaum, Parity breaking effects in diatomic molecules, Zh. Eksp. Teor. Fiz. **75**, 1208 (1978) [Sov. Phys. JETP **48**, 608 (1978)].

[7] L. N. Labzowsky, Λ doubling and parity nonconservation effects in the spectra of diatomic molecules, Zh. Eksp. Teor. Fiz. **75**, 856 (1978) [Sov. Phys. JETP **48**, 434 (1978)].

[8] M. G. Kozlov and L. N. Labzowsky, Topical review: Parity violation effects in diatomics, J. Phys. B **28**, 1933 (1995).

[9] D. DeMille, S. B. Cahn, D. Murphree, D. A. Rahmlow, and M. G. Kozlov, Using Molecules to Measure Nuclear Spin-Dependent Parity Violation, Phys. Rev. Lett. **100**, 023003 (2008).

[10] E. Altuntaş, J. Ammon, S. B. Cahn, and D. DeMille, Demonstration of a Sensitive Method to Measure Nuclear-Spin-Dependent Parity Violation, Phys. Rev. Lett. **120**, 142501 (2018).

[11] A. J. Geddes, L. V. Skripnikov, A. Borschevsky, J. C. Berengut, V. V. Flambaum, and T. P. Rakitzis, Enhanced nuclear-spin-dependent parity-violation effects using the ^{199}HgH molecule, Phys. Rev. A **98**, 022508 (2018).

[12] E. Gajzago and G. Marx, On the weak energy difference between mirror molecules, in *Neutrinos – 1974: Fourth International Conference on Physics and Astrophysics*, edited by H. C. Wolfe and C. Baltay, AIP Conf. Proc. Vol. 22 (AIP, New York, 1974), p. 93.

[13] V. Letokhov, On difference of energy levels of left and right molecules due to weak interactions, Phys. Lett. A **53**, 275 (1975).

[14] O. N. Kompanets, A. R. Kukudzhanov, V. S. Letokhov, and L. L. Gervits, Narrow resonances of saturated absorption of the asymmetrical molecule CHFCIBr and the possibility of weak current detection in molecular physics, Opt. Commun. **19**, 414 (1976).

[15] R. A. Harris and L. Stodolsky, The effect of the parity violating electron–nucleus interaction on the spin–spin coupling Hamiltonian of chiral molecules, J. Chem. Phys. **73**, 3862 (1980).

[16] V. G. Gorshkov, M. G. Kozlov, and L. N. Labzovskii, *P*-odd effects in polyatomic molecules, Zh. Eksp. Teor. Fiz. **82**, 1807 (1982) [Sov. Phys. JETP **55**, 1042 (1982)].

[17] A. Barra and J. Robert, Parity non-conservation and NMR parameters, Mol. Phys. **88**, 875 (1996).

[18] A. Bauder, A. Beil, D. Luckhaus, F. Müller, and M. Quack, Combined high resolution infrared and microwave study of bromochlorofluoromethane, J. Chem. Phys. **106**, 7558 (1997).

[19] V. Weijo, P. Manninen, and J. Vaara, Perturbational calculations of parity-violating effects in nuclear-magnetic-resonance parameters, J. Chem. Phys. **123**, 054501 (2005).

[20] G. Laubender and R. Berger, Electroweak quantum chemistry for nuclear-magnetic-resonance-shielding constants: Impact of electron correlation, Phys. Rev. A **74**, 032105 (2006).

[21] R. Bast, P. Schwerdtfeger, and T. Saue, Parity nonconservation contribution to the nuclear magnetic resonance shielding constants of chiral molecules: A four-component relativistic study, J. Chem. Phys. **125**, 064504 (2006).

[22] V. Weijo, R. Bast, P. Manninen, T. Saue, and J. Vaara, Methodological aspects in the calculation of parity-violating effects in nuclear magnetic resonance parameters, J. Chem. Phys. **126**, 074107 (2007).

[23] S. Nahrwold, R. Berger, and P. Schwerdtfeger, Parity violation in nuclear magnetic resonance frequencies of chiral tetrahedral tungsten complexes NWXYZ (X, Y, Z = H, F, Cl, Br or I), J. Chem. Phys. **140**, 024305 (2014).

[24] J. Eills, J. W. Blanchard, L. Bougas, M. G. Kozlov, A. Pines, and D. Budker, Measuring molecular parity nonconservation using nuclear-magnetic-resonance spectroscopy, Phys. Rev. A **96**, 042119 (2017).

[25] J. W. Blanchard, J. P. King, T. F. Sjolander, M. G. Kozlov, and D. Budker, Molecular parity nonconservation in nuclear spin couplings, Phys. Rev. Res. **2**, 023258 (2020).

[26] E. B. Norrgard, E. R. Edwards, D. J. McCarron, M. H. Steinecker, D. DeMille, S. S. Alam, S. K. Peck, N. S. Wadia, and L. R. Hunter, Hyperfine structure of the $B\,^3\Pi_1$ state and predictions of optical cycling behavior in the $X \rightarrow B$ transition of TlF, Phys. Rev. A **95**, 062506 (2017).

[27] O. Grasdijk, O. Timgren, J. Kastelic, T. Wright, S. Lamoreaux, D. DeMille, K. Wenz, M. Aitken, T. Zelevinsky, T. Winick, and D. Kawall, CeNTREX: A new search for time-reversal symmetry violation in the ^{205}Tl nucleus, Quantum Sci. Technol. **6**, 044007 (2021).

[28] D. Cho, K. Sangster, and E. A. Hinds, Search for time-reversal-symmetry violation in thallium fluoride using a jet source, Phys. Rev. A **44**, 2783 (1991).

[29] V. Flambaum, I. Khriplovich, and O. Sushkov, Nuclear anapole moments, Phys. Lett. B **146**, 367 (1984).

[30] R. v. Boeckh, G. Gräff, and R. Ley, Die abhängigkeit innerer und äußerer wechselwirkungen des TlF-moleküls von der schwingung, rotation und isotopie, Z. Phys. **179**, 285 (1964).

[31] D. A. Wilkening, N. F. Ramsey, and D. J. Larson, Search for *P* and *T* violations in the hyperfine structure of thallium fluoride, Phys. Rev. A **29**, 425 (1984).

[32] J. M. Brown and A. Carrington, *Rotational Spectroscopy of Diatomic Molecules* (Cambridge University Press, Cambridge, UK, 2003).

[33] H. Dijkerman, W. Flegel, G. Gräff, and B. Mönter, Beiträge zum Stark-Effekt der Moleküle ^{205}Tl ^{19}F und ^{39}K ^{19}F, Z. Naturforsch. A **27**, 100 (1972).

[34] M.-A. Bouchiat and C. Bouchiat, Parity violation in atoms, Rep. Prog. Phys. **60**, 1351 (1997).

[35] D. Budker, D. Kimball, D. F. Kimball, and D. P. DeMille, *Atomic Physics: An Exploration through Problems and Solutions*, 2nd ed. (Oxford University Press, Oxford, UK, 2008).

[36] R. Lewis and W. Williams, Parity nonconservation in the hydrogen atom, Phys. Lett. B **59**, 70 (1975).

[37] R. W. Dunford, R. R. Lewis, and W. L. Williams, Parity nonconservation in the hydrogen atom. II, Phys. Rev. A **18**, 2421 (1978).

[38] V. G. Gorshkov, V. F. Ezhov, M. G. Kozlov, and A. I. Mikhailov, P-odd effects in hyperfine transitions in atomic H, K, and Cs, Sov. J. Nucl. Phys. **48**, 867 (1988).

[39] E. Gomez, S. Aubin, G. D. Sprouse, L. A. Orozco, and D. P. DeMille, Measurement method for the nuclear anapole moment of laser-trapped alkali-metal atoms, Phys. Rev. A **75**, 033418 (2007).

[40] M. Bouchiat and C. Bouchiat, I. Parity violation induced by weak neutral currents in atomic physics, J. Phys. France **35**, 899 (1974).

[41] N. Fortson, Possibility of Measuring Parity Nonconservation with a Single Trapped Atomic Ion, Phys. Rev. Lett. **70**, 2383 (1993).

[42] A. T. Nguyen, D. Budker, D. DeMille, and M. Zolotorev, Search for parity nonconservation in atomic dysprosium, Phys. Rev. A **56**, 3453 (1997).

[43] Y. B. Zel'dovich, Electromagnetic interactions with parity-violation, Sov. Phys. JETP **6**, 1184 (1957).

[44] D. L. Bryce and R. E. Wasylishen, Indirect nuclear spin- spin coupling tensors in diatomic molecules: A comparison of results obtained by experiment and first principles calculations, J. Am. Chem. Soc. **122**, 3197 (2000).

[45] M. Olejniczak, R. Bast, T. Saue, and M. Pecul, A simple scheme for magnetic balance in four-component relativistic Kohn-Sham calculations of nuclear magnetic resonance shielding constants in a Gaussian basis, J. Chem. Phys. **136**, 014108 (2012).

[46] M. Iliaš, H. J. A. Jensen, R. Bast, and T. Saue, Gauge origin independent calculations of molecular magnetisabilities in relativistic four-component theory, Mol. Phys. **111**, 1373 (2013).

[47] G. A. Aucar, T. Saue, L. Visscher, and H. J. A. Jensen, On the origin and contribution of the diamagnetic term in four-component relativistic calculations of magnetic properties, J. Chem. Phys. **110**, 6208 (1999).

[48] R. Bast, T. Saue, L. Visscher, H. J. A. Jensen *et al.*, DIRAC, a relativistic *ab initio* electronic structure program, release DIRAC15 (2015), http://www.diracprogram.org.

[49] L. V. Skripnikov, S. Schmidt, J. Ullmann, C. Geppert, F. Kraus, B. Kresse, W. Nörtershäuser, A. F. Privalov, B. Scheibe, V. M. Shabaev *et al.*, New Nuclear Magnetic Moment of ^{209}Bi: Resolving the Bismuth Hyperfine Puzzle, Phys. Rev. Lett. **120**, 093001 (2018).

[50] V. Fella, L. V. Skripnikov, W. Nörtershäuser, M. R. Buchner, H. L. Deubner, F. Kraus, A. F. Privalov, V. M. Shabaev, and M. Vogel, Magnetic moment of ^{207}Pb and the hyperfine splitting of ^{207}Pb^{81+}, Phys. Rev. Res. **2**, 013368 (2020).

[51] L. V. Skripnikov and S. D. Prosnyak, Refined nuclear magnetic dipole moment of rhenium: ^{185}Re and ^{187}Re, Phys. Rev. C **106**, 054303 (2022).

[52] K. G. Dyall, Relativistic double-zeta, triple-zeta, and quadruple-zeta basis sets for the actinides Ac–Lr, Theor. Chem. Acc. **117**, 491 (2007).

[53] K. G. Dyall, Core correlating basis functions for elements 31–118, Theor. Chem. Acc. **131**, 1217 (2012).

[54] K. G. Dyall, Relativistic double-zeta, triple-zeta, and quadruple-zeta basis sets for the light elements H–Ar, Theor. Chem. Acc. **135**, 128 (2016).

[55] C. Adamo and V. Barone, Toward reliable density functional methods without adjustable parameters: The PBE0 model, J. Chem. Phys. **110**, 6158 (1999).

[56] K. P. Huber and G. Herzberg, *Constants of Diatomic Molecules* (Van Nostrand-Reinhold, New York, 1979).

[57] N. J. Stone, Table of nuclear magnetic dipole and electric quadrupole moments, At. Data Nucl. Data Tables **90**, 75 (2005).

[58] L. Visscher and K. G. Dyall, Dirac–Fock atomic electronic structure calculations using different nuclear charge distributions, At. Data Nucl. Data Tables **67**, 207 (1997).

[59] R. Saue, T. Bast, A. S. P. Gomes, H. J. A. Jensen, L. Visscher, I. A. Aucar, R. Di Remigio, K. G. Dyall, E. Eliav, E. Fasshauer, T. Fleig, L. Halbert, E. D. Hedegard, B. Helmich-Paris, M. Ilias, C. R. Jacob, S. Knecht, J. K. Laerdahl, M. L. Vidal, M. K. Nayak, M. Olejniczak *et al.*, The DIRAC code for relativistic molecular calculations, J. Chem. Phys. **152**, 204104 (2020).

[60] M. Kállay, P. R. Nagy, D. Mester, Z. Rolik, G. Samu, J. Csontos, J. Csóka, P. B. Szabó, L. Gyevi-Nagy, B. Hégely, I. Ladjánszki, L. Szegedy, B. Ladóczki, K. Petrov, M. Farkas, P. D. Mezei, and A. Ganyecz, The MRCC program system: Accurate quantum chemistry from water to proteins, J. Chem. Phys. **152**, 074107 (2020).

[61] L. V. Skripnikov, Combined 4-component and relativistic pseudopotential study of ThO for the electron electric dipole moment search, J. Chem. Phys. **145**, 214301 (2016).

[62] L. V. Skripnikov and A. V. Titov, Theoretical study of ThF^+ in the search for T, P-violation effects: Effective state of a Th atom in ThF^+ and ThO compounds, Phys. Rev. A **91**, 042504 (2015).

[63] L. V. Skripnikov and A. V. Titov, Theoretical study of thorium monoxide for the electron electric dipole moment search: Electronic properties of $H^3\Delta_1$ in ThO, J. Chem. Phys. **142**, 024301 (2015).

[64] M. M. Sternheim, Second-order effects of nuclear magnetic fields, Phys. Rev. **128**, 676 (1962).

[65] W. Haxton and C. E. Wieman, Atomic parity nonconservation and nuclear anapole moments, Annu. Rev. Nucl. Part. Sci. **51**, 261 (2001).

[66] V. V. Flambaum and D. W. Murray, Anapole moment and nucleon weak interactions, Phys. Rev. C **56**, 1641 (1997).

[67] S. Gardner, W. Haxton, and B. R. Holstein, A new paradigm for hadronic parity nonconservation and its experimental implications, Annu. Rev. Nucl. Part. Sci. **67**, 69 (2017).

[68] P. A. Vetter, D. M. Meekhof, P. K. Majumder, S. K. Lamoreaux, and E. N. Fortson, Precise Test of Electroweak Theory from a New Measurement of Parity Nonconservation in Atomic Thallium, Phys. Rev. Lett. **74**, 2658 (1995).

[69] N. H. Edwards, S. J. Phipp, P. E. G. Baird, and S. Nakayama, Precise Measurement of Parity Nonconserving Optical Rotation in Atomic Thallium, Phys. Rev. Lett. **74**, 2654 (1995).

[70] W. C. Haxton, C.-P. Liu, and M. J. Ramsey-Musolf, Nuclear anapole moments, Phys. Rev. C **65**, 045502 (2002).

[71] B. M. Roberts, Y. V. Stadnik, V. A. Dzuba, V. V. Flambaum, N. Leefer, and D. Budker, Parity-violating interactions of cosmic fields with atoms, molecules, and nuclei: Concepts and calculations for laboratory searches and extracting limits, Phys. Rev. D **90**, 096005 (2014).

[72] V. A. Dzuba, V. V. Flambaum, and Y. V. Stadnik, Probing Low-Mass Vector Bosons with Parity Nonconservation and Nuclear Anapole Moment Measurements in Atoms and Molecules, Phys. Rev. Lett. **119**, 223201 (2017).

[73] D. Antypas, A. Fabricant, J. E. Stalnaker, K. Tsigutkin, V. V. Flambaum, and D. Budker, Isotopic variation of parity violation in atomic ytterbium, Nat. Phys. **15**, 120 (2019).

[74] http://ckp.nrcki.ru/.

[75] D. A. Varshalovich, A. N. Moskalev, and V. K. Khersonskii, *Quantum Theory of Angular Momentum* (World Scientific, Singapore, 1988).